

PACS numbers: 87.54.Br; 78.20.Hp; 42.62.Be
DOI: 10.1070/QE2002v032n11ABEH002327

Optoacoustic laser monitoring of cooling and freezing of tissues

K.V. Larin, I.V. Larina, M. Motamedi, R.O. Esenaliev

Abstract. **Real-time monitoring of cooling and freezing of tissues, cells, and other biological objects with a high spatial and time resolution, which is necessary for selective destruction of cancer and benign tumours during cryotherapy, as well as for preventing any damage to the structure and functioning of biological objects in cryobiology, is considered. The optoacoustic method, based on the measurement and analysis of acoustic waves induced by short laser pulses, is proposed for monitoring the cooling and freezing of the tissue. The effect of cooling and freezing on the amplitude and time profile of acoustic signals generated in real tissues and in a model object is studied. The experimental results indicate that the optoacoustic laser technique can be used for real-time monitoring of cooling and freezing of biological objects with a submillimeter spatial resolution and a high contrast.**

Keywords: *freezing and cooling of tissues, optoacoustics, optical properties, real-time monitoring.*

1. Introduction

Cryotherapy and local cooling of biological tissues have been used for a long time to treat cancer and benign tumours, muscle spasms, injuries, burns, etc. [1, 2]. At temperatures below the normal body temperature, metabolic reactions in the cells are slowed down or blocked and the vessels contract, thus restricting the supply of oxygen and other substances to the tissues, which are required for a normal functioning of the cell structures. Freezing of tissues leads to a destruction of the cell membranes and cells due to the formation of ice crystals.

All these processes cause necrosis of the tissue. Cryotherapy is used under conditions when surgery and chemotherapy can lead to complications, especially in organs like liver, kidneys, brain and prostate. However, large-scale clinical application of cryotherapy is restricted due to the absence of a method for real-time monitoring the cooling and freezing of tissues with a sufficient resolution and contrast.

K.V. Larin, I.V. Larina, M. Motamedi, R.O. Esenaliev University of Texas, Medical Branch, MS 0456, 301 University Boulevard, Galveston, Texas 77555-0456; Tel.: (409)-772-8144, fax: (409)-772-8384; e-mail: rinat.esenaliev@utmb.edu

Received 4 September 2002
Kvantovaya Elektronika **32** (11) 953–958 (2002)
Translated by Ram Wadhwa

Cooling and freezing of tissues are employed not only in cryotherapy, but also in cryobiology for preserving organs, tissues and other biological objects [3, 4]. Real-time monitoring of cooling and freezing of tissues with a high spatial and time resolution is necessary for freezing biological objects to the required temperature at a cooling rate that makes it possible to preserve their normal structure and functioning.

Several methods have been proposed in recent years for monitoring the freezing of tissues during cryotherapy, including ultrasonic and computer tomography [5–8], as well as NMR [9, 10]. Each of these methods has its own advantages. However, their application is limited due to an insufficient resolution and contrast, high cost, or a long time required for measuring and processing of signals [11].

We proposed an optoacoustic method for real-time monitoring of the cooling and freezing of tissues with a high contrast and resolution [12]. This method is based on the detection and analysis of laser-induced acoustic waves generated by the thermoelastic mechanism [13] and containing information about optical and thermal properties of the tissue. Optoacoustics has been developed extensively in the last years for medical diagnostics [14–21]. Investigations show that the optoacoustic method has a number of advantages (a deeper detection level, a higher contrast of the obtained images, and a higher resolution) over optical or ultrasonic methods. *In vivo* and *in vitro* studies of real biological tissues and model tissues have revealed that this method provides a high contrast and resolution.

In this work, we study the possibility of real-time optoacoustic monitoring of cooling and freezing of a biological tissue (liver) and a model biological object (aqueous solution of potassium chromate) with a high resolution.

2. Theory

The absorption of a short light pulse in a medium is accompanied by nonradiative relaxation, which leads to heating and generation of an acoustic pressure pulse. The distribution of the acoustic pressure in an absorbing nonscattering medium is described by the expression [13]

$$P(z) = \frac{\beta c_s^2}{C_p}\mu_a F(z) = \Gamma\mu_a F(z) = \Gamma\mu_a F_0 e^{-\mu_a z}, \quad (1)$$

where β is the thermal expansion coefficient (K^{-1}); c_s is the sound speed in the medium (cm s^{-1}); C_p is the specific heat at constant pressure (J g^{-1} K^{-1}); μ_a is the absorption

coefficient (cm^{-1}); $F(z)$ is the laser power density in the medium (J cm^{-2}); F_0 is the power density of the incident laser radiation (J cm^{-2}); and

$$\Gamma = \frac{\beta c_s^2}{C_p} \tag{2}$$

is the Grüneisen coefficient. One can see from expression (1) that the absorption coefficient of a nonscattering medium determines the exponential slope (exponent) of the acoustic pressure pulse distribution in the medium.

For objects that not only absorb light but also scatter it strongly, the exponent is determined by the effective attenuation coefficient μ_{eff} [22]:

$$\mu_{eff} = \left[3\mu_a(\mu_a + \mu_s')\right]^{1/2}, \tag{3}$$

where $\mu_s' = \mu_s(1-g)$ is the reduced (or transport) scattering coefficient (cm^{-1}); μ_s is the scattering coefficient (cm^{-1}); and g is the dimensionless factor of scattering anisotropy [22], which can take values between 0 and 1: $g = 0$ corresponds to isotropic (e.g., Rayleigh) scattering, and $g = 1$ to total forward scattering.

Thus, the distribution of acoustic pressure in a biological tissue with the effective attenuation coefficient μ_{eff} can be written in the form

$$P(z) = \Gamma\mu_a k F_0 e^{-\mu_{eff} z}, \tag{4}$$

where k is a coefficient depending on the optical properties of the biological tissue.

Parameters z and t are related through the sound speed

$$z = c_s t, \tag{5}$$

hence the temporal profile of the increasing exponential part of the acoustic signal has the following form in the case of direct detection [23]:

$$P(t) = \Gamma\mu_a k F_0 e^{-\mu_{eff} c_s t}. \tag{6}$$

Our previous study has shown that the Grüneisen coefficient of the biological tissue depends linearly on temperature T in the interval 20–52 °C [24]:

$$\Gamma = A + BT, \tag{7}$$

where A and B are constants. Therefore, expression (6) can be presented in the form

$$P(t) = \left[A + BT(t)\right] k\mu_a F_0 e^{-\mu_{eff} c_s t}. \tag{8}$$

It follows from (8) that the amplitude and the exponential slope (defined as $\mu_{eff} c_s$) of the acoustic signal in tissues depend on their temperature, optical and thermal properties, as well as on the sound speed. This peculiarity of acoustic waves was used for real-time monitoring of the heating [24, 25] and coagulation [26] of biological tissues with a high contrast and resolution.

It can be expected that the Grüneisen coefficient decreases linearly upon cooling of the biological tissue from 20 °C to the freezing temperature. Moreover, the exponential profile of the acoustic signal may vary significantly upon freezing of the tissue due to a variation of the optical properties and the sound speed in it.

3. Experimental

3.1 Coolant

Liquid nitrogen (condensation temperature −196 °C), used widely for freezing biological tissues in cryotherapy and cryobiology, was employed as the coolant in our experiments. Liquid nitrogen was poured from above on the samples covered by a quartz plate, which prevented a direct contact of the samples with liquid nitrogen, permitted their exposure to laser pulses, and also provided a rigid boundary for acoustic signal generation.

3.2 Model object and biological tissue

Aqueous solution of potassium chromate (K_2CrO_4) was used as the model object. This solution has a high stability and absorbs radiation in the visible and ultraviolet spectral regions. The absorption coefficient μ_a of the solution used in the experiment was 100 cm^{-1} at the third-harmonic wavelength 355 nm of a Nd : YAG laser. The solution was held in a special cell covered by a quartz plate to prevent a direct contact with liquid nitrogen (see Fig. 1). The thickness of the aqueous solution in the cell was 1 mm.

Experiments with the biological tissue were carried out on a dog's liver removed immediately after euthanasia. The choice of the biological tissue was dictated by the fact that cryotherapy is frequently employed for treating liver tumours resulting from possible severe haemorrhage accompanying the surgical extraction of tumours, as well as by a low efficiency of chemotherapy. Moreover, metastatic liver tumour is one of the main reasons behind the death of patients suffering from the cancer of the gastrointestinal tract. The biological tissue samples had a thickness of 2–3 cm and were placed directly on the acoustic detector. The tissue was covered from the side by a thin polymer film to prevent its drying and direct contact with liquid nitrogen. As in the experiments with an absorbing solution, the biological tissue was covered from above by a quartz plate.

3.3 Laser source

The experimental setup for optoacustic monitoring of cooling and freezing of biological tissues and model samples is shown in Fig. 1. The 1064-nm first harmonic of a Nd : YAG laser was used for irradiating the liver tissue. Radiation at this wavelength penetrates most deeply into

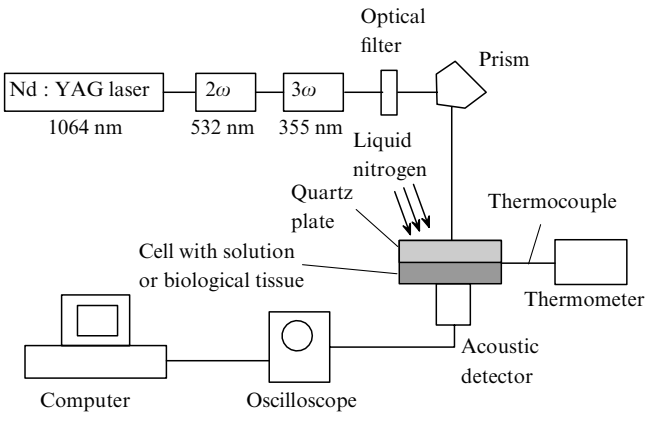

Figure 1. Scheme of the experimental setup for monitoring the cooling and freezing of model and real biological tissues.

the biological tissue [22]. For this reason, the first harmonic of the Nd : YAG laser is used frequently in laser diagnostics and therapy. The 335-nm third harmonic of the Nd : YAG laser was used for irradiating the aqueous solution of potassium chromate. The energy of laser pulses was measured with a calibrated power meter. Typical values of the energies of incident radiation were 15 and 2 mJ at 1064 and 355 nm, respectively. This provided an energy density of 30 and 4 mJ cm^{-2} for incident laser pulses at 1064 and 355 nm, respectively, and a laser beam of diameter 8 mm. The duration of laser pulses was 10 ns.

3.4 Detecting and recording system

Acoustic waves were measured with broadband piezoelectric detectors. Acoustic waves generated in the liver tissue were measured with a PVDF piezoelectric detector (passband 0.1 – 5 MHz), while acoustic waves generated in an absorbing solution were measured with a PZT-5 piezoelectric detector (passband 0.5 – 50 MHz). The acoustic signals were amplified with the help of a broadband preamplifier. The signal from the preamplifier was displayed on an oscilloscope and processed with a PC.

3.5 Sample temperature measurement

We measured the sample temperature in our experiments with a thermocouple mounted on the upper surface of the samples. The signal from the thermocouple was detected with a Scanner Plus digital calibrated thermometer.

4. Results

Fig. 2 shows the temperature dependence of the coefficient of thermal expansion of water in the temperature range 0 – 20 °C [27]. The thermal expansion coefficient in this range almost linearly depends on temperature and is equal to zero at 3.9 °C.

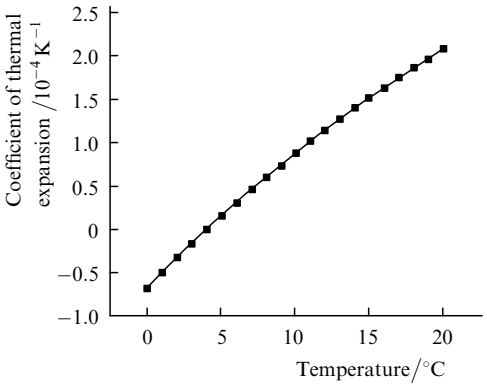

Figure 2. Thermal expansion coefficient of water in the temperature range 0 – 20 °C.

The coefficient of thermal expansion of water is negative in the temperature range 0 – 3.9 °C. Due to this unique property, water contracts upon heating in this temperature range, and hence the Grüneisen coefficient Γ is also negative in the interval from 0 to 3.9 °C. At $T > 3.9$ °C, the Grüneisen coefficient is positive. Due to such a temperature dependence of the thermal expansion coefficient and of the Grüneisen coefficient, acoustic pressure with a positive sign (expansion of water) is generated in water, while the acoustic pressure in the interval $T = 0 - 3.9$ °C is negative (contraction of water) [28]. In the range 0 – 20 °C, the sound speed and the specific heat of water do not change significantly. Ice has a positive thermal expansion coefficient, and hence one can expect a positive acoustic pressure generation in the frozen liver and in the absorbing solution.

Fig. 3 shows typical acoustic signals obtained in experiments with aqueous solutions of potassium chromate at temperatures 25.5, 1.3 and −10 °C. The signals measured in the aqueous solution are plotted on the inverted time scale, and $t = 0$ corresponds to the solution – quartz interface. Such a representation of signals is used frequently for a more clear demonstration of the acoustic pressure distribution in the irradiated medium [23]. One can see from Fig. 3 that the amplitude and the exponential slope of the acoustic signal measured in ice ($T = -10$ °C) are much higher than the corresponding values of these parameters measured in water ($T = 25.5$ °C). Moreover, the signal measured in water at $T = 1.3$ °C has a negative amplitude.

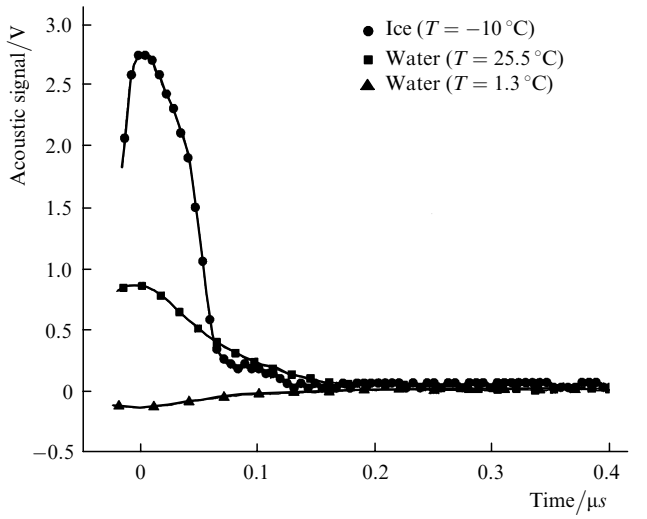

Figure 3. Acoustic signals obtained in the aqueous solution of potassium chromate during cooling and freezing.

Fig. 4 shows the temperature dependence of the acoustic signal amplitude obtained in aqueous solutions of potassium chromate at temperatures between 24 and −11 °C. The amplitude of the acoustic signals decreases almost linearly upon cooling down to 0 °C. This part of the curve corresponds to water in the liquid state. The second part of the curve (for temperatures below 0 °C) corresponds to the data obtained for water in the solid (frozen) state. The amplitude of the acoustic signal induced in the sample at temperatures below 0 °C increases with decreasing temperature. A negative acoustic pressure was observed in the temperature range 0 – 3.5 °C. This is in good agreement with the theoretical data on the temperature dependence of the thermal expansion coefficient of water presented in Fig. 2, as well as with the experimental results obtained by other researchers [28, 29]. The plot for the absorbing solution presented in Fig. 4 has two experimental points at 0 °C because the acoustic signal was generated in both the solid and liquid phases of water.

The temperature dependence of the exponential slope of acoustic signals measured in the aqueous solution of

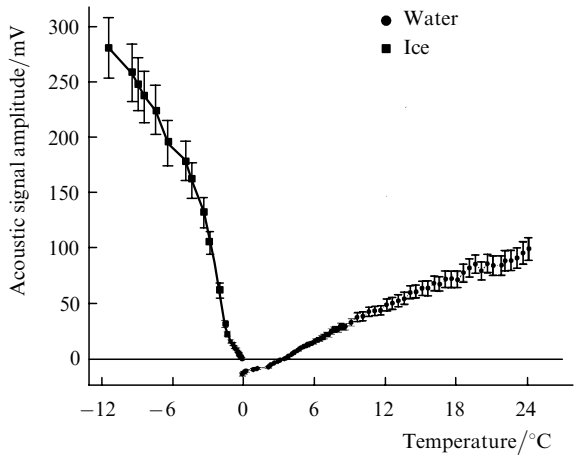

Figure 4. Amplitude of the acoustic signals measured in the aqueous solution of potassium chromate during cooling and freezing.

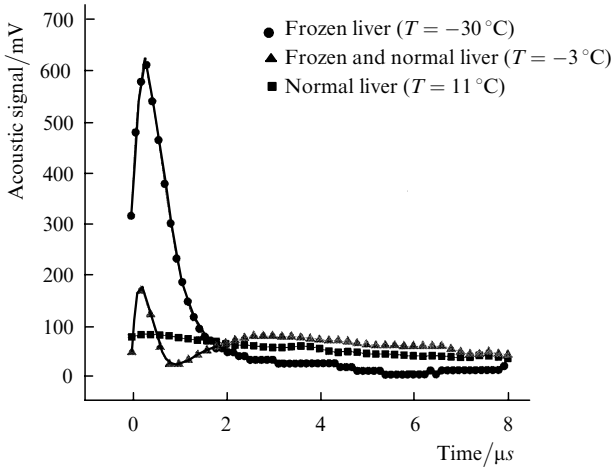

Figure 6. Acoustic signals obtained from the normal, partially frozen and completely frozen liver.

potassium chromate during cooling and freezing is presented in Fig. 5. The plot can be divided into three regions: from 24 °C to about 0 °C, from 0 °C to −8 °C, and below −8 °C. These regions correspond to the solution in the liquid state, partially liquid and partially solid state, and completely solidified state, respectively. The exponential slope of the acoustic signals remains constant (to within 10 % error of measurements) in the temperature range 24 – 0 °C because the optical properties and the sound speed change insignificantly at such temperatures. A sharp increase in the exponential slope of acoustic signals in the temperature range from −2 to −8 °C is caused by the formation of a frozen layer in the absorbing solution. At temperatures below −8 °C, the slope of the acoustic signal is relatively constant and is higher than the slope measured at positive temperatures.

Fig. 6 shows typical acoustic signals obtained in the experiments with the normal and frozen liver tissue at temperatures 11, −3, and −30 °C. The data presented in the figure show that the acoustic signals generated in the biological tissue depend strongly on temperature. The amplitude and exponential slope of the signal measured in the frozen tissue (at −30 °C) are much larger than the corresponding values measured in the normal tissue (at 11 °C). The acoustic signal measured at a temperature −3 °C has two peaks. The first peak is generated in the frozen part of the biological tissue, and the second peak in the normal part that is not frozen.

The amplitude of the acoustic signals generated in the biological tissue at various temperatures is presented in Fig. 7. One can see that the amplitude decreases upon cooling right down to −3 °C, and increases sharply at lower temperatures. The dependence in the transient region between normal and frozen biological tissue (from −2 to −3 °C) is ambiguous. This is due to the fact that the acoustic signal has two peaks, one induced in the frozen zone of the tissue and the other in the zone not yet frozen.

The slopes of the acoustic signals obtained in the liver tissue at different temperatures are shown in Fig. 8. Like the plot for the absorbing solution (see Fig. 5), the curve can be divided into three regions: from 20 to −2 °C, from −2 to −4 °C, and below −4 °C. These regions correspond to the

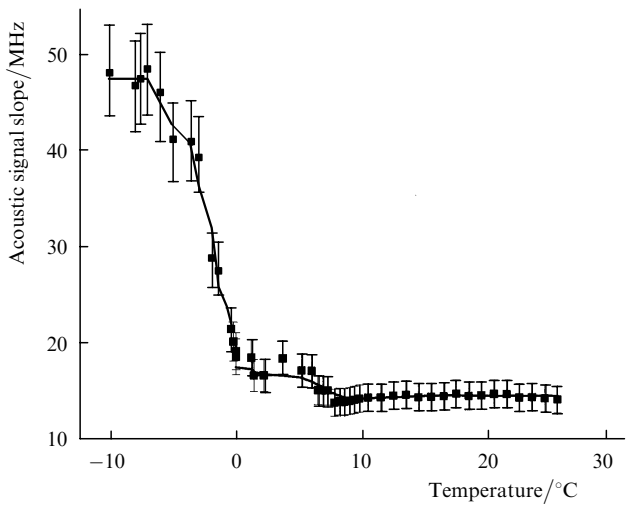

Figure 5. Exponential slope of the acoustic signals measured in the aqueous solution of potassium chromate during cooling and freezing.

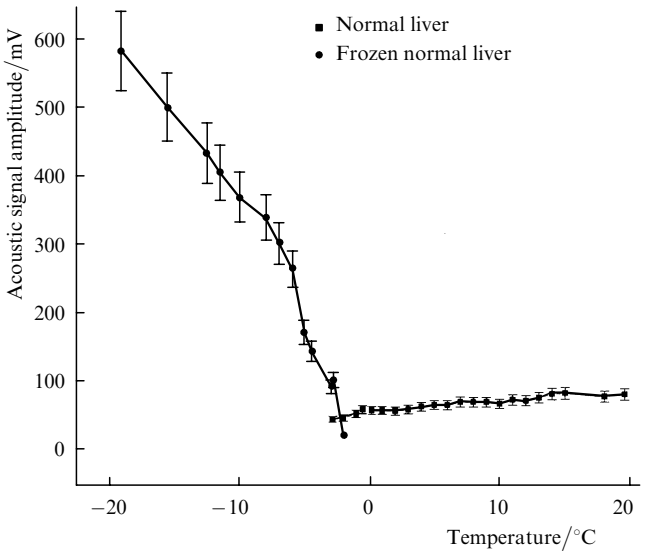

Figure 7. Amplitude of the acoustic signals measured in the liver tissue during cooling and freezing.

normal tissue, tissue comprised of normal and frozen components, and completely frozen tissue. The exponential slope of acoustic signals remains constant in the temperature range from 20 to $-2\,^{\circ}C$ due to the fact that the optical properties and the sound speed in the liver change insignificantly at such temperatures. A sharp increase in the exponential slope of acoustic signals in the temperature range from -2 to $-4\,^{\circ}C$ is caused by the formation of a frozen layer in the liver tissue. At temperatures below $-4\,^{\circ}C$, the slope of the acoustic signal is relatively constant and is 45 times larger than the slope measured in the normal tissue.

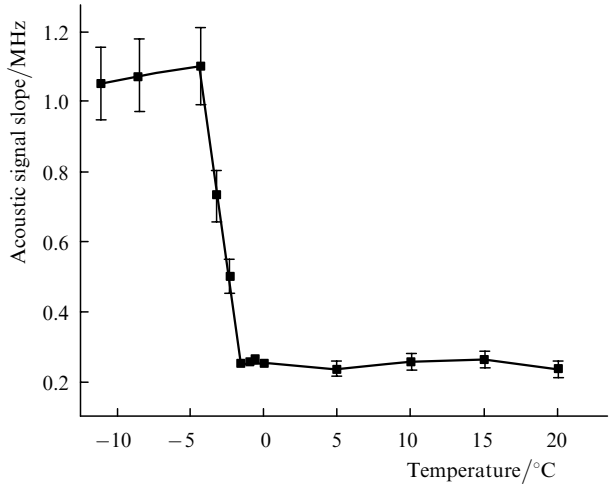

Figure 8. Exponential slope of the acoustic signals measured in the liver tissue during cooling and freezing.

An analysis of the signals obtained from the liver tissue allowed us to calculate the thickness of the frozen zone produced upon cooling of the tissue by liquid nitrogen. The thickness of the frozen zone was calculated as the product of the duration of the acoustic signal generated in the frozen zone and the sound speed in the frozen tissue. Fig. 9 shows the thickness of the frozen zone at various temperatures measured by a thermocouple. The high resolution of the optoacoustic technique allowed us to measure the thickness of the frozen zone with a resolution not worse than 0.5 mm. It was found to be equal to 1.1 mm at a temperature of $-2\,^{\circ}C$ and 3 mm at $-10\,^{\circ}C$.

5. Discussion of results

The slope of the acoustic signals measured in the liver tissue (Fig. 8) does not change at temperatures between 20 and $-2\,^{\circ}C$. This is due to the fact that the sound speed and the optical properties of the biological tissue do not change at these temperatures. The slope measured in a completely frozen biological tissue is virtually temperature-independent, but its magnitude is about 4–5 times higher than the slope measured in the normal tissue. The discrepancy in the absolute values is explained by the fact that the sound speed is equal to about 1.5×10^5 cm s^{-1} in water and 4.0×10^5 cm s^{-1} in ice, while the effective attenuation coefficient is equal to 1.9 and 3.2 cm^{-1} for the frozen and normal liver tissue, respectively [22]. A sharp increase in the slope of the acoustic signal between -2 and $-4\,^{\circ}C$ is caused by the formation of the frozen zone in the biological tissue.

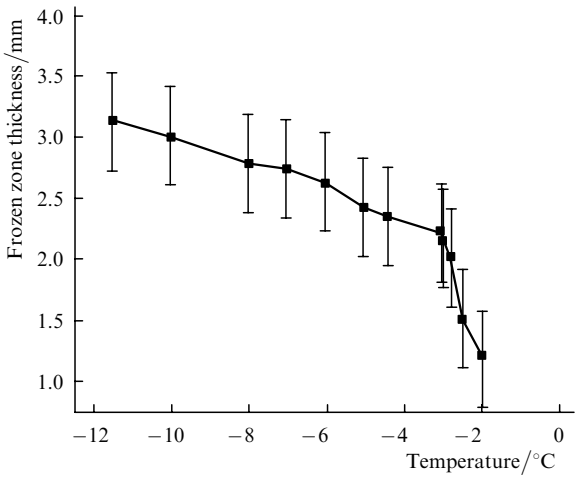

Figure 9. Temperature dependence of the thickness of the frozen zone of the liver tissue.

The data presented in Fig. 9 demonstrate a high resolution (not worse than 0.5 mm) of the optoacoustic method. Such a resolution is sufficient for monitoring the freezing of biological objects with a high degree of precision. However, the resolution can be improved further by using acoustic detectors with a broader passband and a recording system with a higher time resolution.

We have performed real-time measurements of the acoustic signals. Therefore, the optoacoustic method can be used for real-time monitoring of cooling and freezing of tissues in cryotherapy and cryobiology.

One- and two-dimensional arrays of piezoelements can be used for obtaining two- and three-dimensional images of frozen and cooled tissues.

Exposure of the absorbing media to short optical pulses leads to a heating of these media and hence to the generation of a positive acoustic pressure. The results of our experiments carried out in aqueous solution have demonstrated a unique feature of negative acoustic pressure generation in the temperature range between zero and about $4\,^{\circ}C$. Irradiation of water by short laser pulses in this temperature range leads to a contraction of water [22, 29]. Because water has a negative thermal expansion coefficient (and hence a negative Grüneisen coefficient) in the temperature range between zero and about $4\,^{\circ}C$, we recorded negative acoustic pressure at these temperatures.

6. Conclusions

Our study has shown that the amplitude of acoustic signals generated in the biological tissue and in a model biological object depends on temperature. The amplitude and slope of these signals increase sharply upon freezing of the biological tissue and the model biological object. The optoacoustic technique allows real-time monitoring of the temperature variation and the frozen-zone formation. This method can be used to measure the thickness of the frozen zone with a spatial resolution of no less than 0.5 mm. Thus, the optoacoustic method can be used for monitoring the cooling and freezing of tissues in cryotherapy and in cryobiology.

Acknowledgements. This work was supported by Whitaker Foundation.

References

1. Lehmann J.F. *Therapeutic Heat and Cold* (Baltimore – Hong Kong – London – Sidney, 1990).
2. Fuller B.J., Grout W.W. *Clinical Applications of Cryobiology* (Boca Raton: CRC Press, 1991).
3. Dobrinsky J.R. *Theriogenology*, **57** (1), 285 (2002).
4. Diller K.R. *Cryobiology*, **34** (4), 304 (1997).
5. Gilbert J.C., Onik G.M., Hoddick W.K., Rubinsky B. *Cryobiology*, **22** (4), 319 (1985).
6. Laugier P., Berger G. *Ultrasonic Imaging*, **15** (1), 14 (1993).
7. Sandison G.A., Loye M.P., Rewcastle J.C., et al. *Physics in Medicine & Biology*, **43** (11), 3309 (1998).
8. Saliken J.C., McKinnon J.G., Gray R. *American J. of Roentgenology*, **166** (4), 853 (1996).
9. Matsumoto R., Selig A.M., Colucci V.M., Jolesz F.A. *J. of Magnetic Resonance Imaging*, **3** (5), 770 (1993).
10. Matsumoto R., Oshio K., Jolesz F.A. *J of Magnetic Resonance Imaging*, **2** (5), 555 (1992).
11. Tacke J., Speetzen R., Heschel I., Hunter D.W., Rau G., Gunther R.W. *Cryobiology*, **38** (3), 250 (1999).
12. Larina I.V., Larin K.V., Motamedi M., Esenaliev R.O. *Proc. SPIE Int. Soc. Opt. Eng.*, **4001**, 361 (2000).
13. Gusev V.E., Karabutov A.A. *Lazernaya optoakustika* (Laser Optoacoustics) (Moscow: Nauka, 1993).
14. Esenaliev R.O., Oraevsky A.A., Letokhov V.S., Karabutov A.A., Malinsky T.V. *Lasers in Surgery and Medicine*, **13**, 470 (1993).
15. Oraevsky A.A., Jacques S.L., Esenaliev R.O., Tittel F.K. *Proc. SPIE Int. Soc. Opt. Eng.*, **2134**, 122 (1994).
16. Esenaliev R.O., Karabutov A.A., Tittel F.K., Fornage B.D., Thomsen S.L., Stelling C., Oraevsky A.A. *Proc. SPIE Int. Soc. Opt. Eng.*, **2979**, 71 (1997).
17. Oraevsky A.A., Andreev V.G., Karabutov A.A., Esenaliev R.O. *Proc. SPIE Int. Soc. Opt. Eng.*, **3601**, 256 (1999).
18. Esenaliev R.O., Larina I.V., Larin K.V., Motamedi M., Karabutov A.A., Oraevsky A.A. *Proc. SPIE Int. Soc. Opt. Eng.*, **3594**, 101 (1999).
19. Esenaliev R.O., Karabutov A.A., Oraevsky A.A. *IEEE J. of Selected Topics in Quantum Electron.*, **5** (4), 981 (1999).
20. Larin K.V., Hartrumpf O., Larina I.V., Esenaliev R.O. *Proc. SPIE Int. Soc. Opt. Eng.*, **4256**, 147 (2001).
21. Esenaliev R.O., Larina I.V., Larin K.V., Deyo D.E., Motamedi M., Prough D.S. *Appl. Opt.*, **41** (22), 4722 (2002).
22. Welch A.J., van Gemert M.J.C. *Optical-Thermal Response of Laser-Irradiated Tissue* (New York: Plenum Press, 1995).
23. Karabutov A.A., Podymova N.B., Letokhov V.S. *Appl. Phys. B*, **63**, 545 (1996).
24. Esenaliev R.O., Oraevsky A.A., Larin K.V., Larina I.V., Motamedi M. *Proc. SPIE Int. Soc. Opt. Eng.*, **3601**, 268 (1999).
25. Larin K.V., Larina I.V., Motamedi M., Esenaliev R.O. *Proc. SPIE Int. Soc. Opt. Eng.*, **3916**, 311 (2000).
26. Esenaliev R.O., Larina I.V., Larin K.V., Motamedi M. *Proc. SPIE Int. Soc. Opt. Eng.*, **3916**, 302 (2000).
27. Gray D.E. *American Institute of Physics Handbook* (McGraw-Hill Book Co., 1972).
28. Dunina T.A., Egerev S.V., Naugol'nykh K.A. *Pis'ma Zh. Tekh. Fiz.*, **9**, 410 (1983).
29. Sigrist M.W. *J. Appl. Phys.*, **60**, R83 (1986).